Longitudinal Assessment of Subcortical Gray Matter Volume, Cortical Thickness, and White Matter Integrity in HIV-Positive Patients

Diogo Goulart Corrêa,[1,2]* Nicolle Zimmermann,[1,3] Gustavo Tukamoto,[2] Thomas Doring,[2] Nina Ventura,[1,2] Sarah C.B. Leite,[1] Rafael Ferracini Cabral,[1] Rochele Paz Fonseca,[1,3] Paulo R.V. Bahia,[1] and Emerson Leandro Gasparetto[1,2]

Purpose: To longitudinally evaluate the cortical thickness and deep gray matter structures volume, measured from T1 three-dimensional (3D) Gradient echo-weighted imaging, and white matter integrity, assessed from diffusion tensor imaging (DTI) of HIV-positive patients.
Materials and Methods: Twenty-one HIV-positive patients on stable highly active antiretroviral therapy (HAART) with CD4+ T lymphocytes count >200 cells/mL and viral load <50 copies/mL underwent two magnetic resonance imaging (MRI) scans with a median interval of 26.6 months. None of the patients had HIV-related dementia. T1 3D magnetization prepared rapid gradient echo-weighted imaging and DTI along 30 noncolinear directions were performed using a 1.5 Tesla MR scanner. FreeSurfer was used to perform cortical volumetric reconstruction and segmentation of deep gray matter structures. For tract-based spatial statistics analysis, a white matter skeleton was created, and a permutation-based inference with 5000 permutations, with a threshold of $P < 0.05$ was used to identify abnormalities in fractional anisotropy (FA). The median, radial, and axial diffusivities were also projected onto the mean FA skeleton.
Results: There were no significant differences in cortical thickness, deep gray matter structures volumes or diffusivity parameters between scans at the two time points (considering $P < 0.05$).
Conclusion: No longitudinal differences in cortical thickness, deep gray matter volumes, or white matter integrity were observed in an HIV-positive population on stable HAART, with undetectable viral load and high CD4+ T lymphocytes count.

J. MAGN. RESON. IMAGING 2016;00:000–000.

Human immunodeficiency virus (HIV) arrives at the central nervous system (CNS) early in the course of infection, even in the pre-acquired immune deficiency syndrome phase.[1] Clinically relevant CNS symptoms are observed in more than 50% of patients who do not receive highly active antiretroviral therapy (HAART).[2] HIV infection was initially uniformly fatal; today, it can be treated effectively by HAART.[3] The introduction of HAART profoundly decreased morbidity and mortality in the HIV-positive population, reducing the prevalence of opportunistic infections.[2] Unfortunately, HIV-associated neurocognitive disorders (HAND) remain frequent.[2,4] HAND may be undiagnosed due to no or mild symptoms,[2,5] but they impact daily functioning and predict non-CNS morbidity and mortality.[2] In addition, the prevalence of asymptomatic and mild neurocognitive disorder has been unchanged by HAART, suggesting that HAND continue in the antiretroviral era.[5]

Neuroimaging plays an important role in diagnosing opportunistic infections in HIV-positive patients, but has limited utility in the evaluation of HAND.[6] Ideally, to benefit HAND diagnosis, a neuroimaging method should diagnose HIV-related CNS injury, detect presymptomatic changes due

View this article online at wileyonlinelibrary.com. DOI: 10.1002/jmri.25263

Received Jan 31, 2016, Accepted for publication Mar 18, 2016.

*Address reprint requests to: D.G.C., Hospital Universitário Clementino Fraga Filho, Rua Rodolpho Paulo Rocco 255, Cidade Universitária, Ilha do Fundão, Rio de Janeiro, RJ, 21941913, Brazil. E-mail: diogogoulartcorrea@yahoo.com.br

From the [1]Department of Radiology, Hospital Universitário Clementino Fraga Filho, Federal University of Rio de Janeiro, Cidade Universitária, Ilha do Fundão, Rio de Janeiro, RJ, Brazil; [2]Clínica de Diagnóstico por Imagem (CDPI), Barra da Tijuca, Rio de Janeiro, RJ, Brazil; and [3]Department of Psychology, Pontifical Catholic University of Rio Grande do Sul, Partenon, Porto Alegre, RS, Brazil.

to HIV, and assess treatment effects.[2] On T2-weighted MRI, HIV-associated dementia (HAD) is characterized by cerebral atrophy with or without periventricular white matter hyperintensities, which are diffuse, largely symmetric, and not characterized by edema or mass effect.[6] However, these findings are not specific for HAD, especially in its earlier stages, and they may be observed in neuroasymptomatic HIV-infected patients.[6]

Previous studies showed that advanced neuroimaging techniques, such as diffusion tensor imaging (DTI),[7] measurement of cortical thickness,[8] and measurement of deep gray matter volumes,[9] detect changes in HIV-infected patients earlier than conventional MRI.

DTI is an imaging modality that measures anisotropy, or the directional nature of water diffusion through cellular structures, such as myelin and white matter tracts, which can differ between normal and pathological tissue.[10] Most previous studies have found decreased fractional anisotropy (FA) and increased mean diffusivity (MD) and radial diffusivity (RD) in white matter regions of HIV-infected patients.[11–19] Quantitative measurements of basal ganglia volume and cortical thickness in HIV-positive patients showed significant differences relative to controls.[8,9,20–25] However, there is a large overlap of values between patients and controls,[7,14] which prevents the use of these techniques in clinical practice.

Because advanced MRI techniques can detect early differences between HIV-positive patients and controls, they might also show premature deterioration of white matter integrity or reduction in cortical thickness and deep gray matter volume, in a longitudinal study within HIV-positive patients. These data could be used to make changes in antiretroviral drug therapy and/or nonpharmacological approaches, such as cognitive therapy, with the goal of improving the quality of life of these patients.

The objective of this study is to longitudinally evaluate the integrity of the white matter, by DTI, the cortical thickness and deep gray matter structures (basal ganglia, thalami and hippocampi) volumes, using voxels-based techniques, in HIV-infected patients.

Materials and Methods

Subjects

The Institutional Review Board approved this study, and all participants signed an informed consent. Between September 2009 and May 2014, 21 patients with HIV infections, confirmed by enzyme-linked immunosorbent assay and Western blot, were randomly selected from the University Hospital database. On the week of the first MRI, all patients were on stable HAART and had viral load <50 copies/mL and CD4+ T lymphocyte >200 cells/mL. Exclusion criteria included neurological disorders, current or past CNS infection, contraindications to MRI, abnormal findings on MRI in conventional sequences, and discontinuation of HAART. The group included 18 men and 3 women (mean age, 52.9 years; range, 44 to 61 years) with an average of 10.2 years of education (range, 4 to 20 years). All patients had at least 5 years of known HIV-infection with an average of 14.0 years of illness (range, 5 to 24 years) and a median of 678.4 CD4+ T lymphocytes cells/mL (range, 264 to 1164 cells/mL). According to the American Centers for Disease Control and Prevention (CDC), of the 21 patients, 6 patients were classified as A1, 2 as A2, 1 as A3, 2 as B2, 2 as B3, 4 as C2, and 4 as C3. All patients were receiving HAART (Table 1). Based on the Memorial Sloan Kettering (MSK) Ratio Scale,[4] 19 patients were rated as 0.0, 1 was rated as 0.5, 1 was rated as 1.0, and none was rated as 2.0 or greater.

A neuropsychological tests battery based on Antinori et al[4] was used to characterize the cognitive profiles of all participants on the day of the first MRI. Tests were administered by a trained neuropsychologist with 8 years of experience, who was blinded to the imaging results. The battery consisted of standard tests, which were adapted and interpreted according to normative demographic data from a Brazilian population. Raw scores from neuropsychological tests were transformed into Z scores using the following formula: patient raw score minus normative mean divided by normative standard deviation. Impairment was defined as mean Z score $\leq$ -1.5. Lower Z scores represented more severe impairment, except in tests of processing speed, for which a lower score represented less time to complete the task. All cognitive domains, respective neuropsychological tests and specific variables evaluated are shown in Table 2.

Of the 21 patients, 9 did not have HAND, 10 had HIV-associated asymptomatic neurocognitive impairment, 2 had HIV-associated mild neurocognitive disorder, and none had HAD, according to Antinori et al.[4] Ten patients had deficits in memory, five in processing speed, three in executive function, two in attention/working memory, two in verbal language, and one in motor and sensory-perceptual skills.

All participants underwent two MRIs with an average interval of 26.6 months (range, 12 to 37 months). At the time of the second MRI, all patients remained on the same antiretroviral regimen, maintaining CD4+ T lymphocyte count >200 cells/mL, undetectable plasma viral load and the same MSK rating scale.

MRI Acquisition

The MRI was acquired on a 1.5 Tesla (T) scanner (Avanto, Siemens, Erlangen, Germany), using an eight-channel phased-array head coil. The MRI protocol included: axial FLAIR (repetition time [TR], 9000 ms; echo time [TE], 83 ms; field of view [FOV], 230 mm; matrix, 244 × 256; section thickness, 4.5 mm with a 10% gap; flip angle 180°; inversion time, 2500 ms); sagittal T1 3D magnetization prepared rapid gradient echo (MPRAGE)-weighted image (TR, 2730 ms; TE, 3.26 ms; inversion time, 1000 ms; FOV, 256 mm; matrix, 192 × 256; 1.3 mm section thickness, flip angle, 7°; voxel size, 1.3 mm × 1.0 mm × 1.3 mm), and axial diffusion tensor single-shot echo-planar imaging was acquired using bipolar diffusion gradients applied along thirty noncolinear directions (b0 = 0 and b1 = 900 s/mm^2) (TR, 10100 ms; TE, 94 ms; FOV, 256 mm; matrix, 122 × 120; 65 slices with 2.1 mm thickness and no gap). Subjects' heads were stabilized with tape across the forehead and padding around the sides. All MRIs were

TABLE 1. Antiretroviral Schemes Used by the Participants and the CNS Penetration-Effectiveness Score

Antiretroviral therapy	No. of patients using the scheme	CNS penetration-effectiveness score[26]
Zidovudine + lamivudine + efavirenz	6	9
Zidovudine + lamivudine + atazanavir/ritonavir	3	8
Zidovudine + lamivudine + tenofovir + efavirenz	1	10
Zidovudine + lamivudine + fosamprenavir/ritonavir	1	9
Zidovudine + lamivudine + tenofovir + lopinavir/ritonavir	1	10
Zidovudine + lamivudine + tenofavir + lopinavir/ritonavir	1	10
Abacavir + lamivudine + atazanavir/ritonavir	1	7
Tenofovir + lamivudine + efavirenz	1	6
Lamivudine + tenofovir + efavirenz	1	6
Zidovudine + tenofovir + lamivudine + lopinavir/ritonavir	1	10
Zidovudine + lamivudine + tenofovir + lopinavir/ritonavir	1	10
Zidovudine + tenofovir + darunavir/ritonavir	1	8
Lamivudine + tenofovir + fosamprenavir/ritonavir	1	8
Lamivudine + tenofovir + lopinavir/ritonavir + raltegravir + enfuvirtide	1	10

reviewed by a neuroradiologist (E.L.G., 15 years of experience) and were of good quality for postprocessing.

Cortical Thickness, Volumetric Measures, and Statistical Analysis

Cortical reconstruction and volumetric segmentation was performed using FreeSurfer version 5.0.0 (http://surfer.nmr.mgh.harvard.edu), using the sagittal T1 3D MPRAGE-weighted image. Technical details of these procedures have been described previously.[27] Briefly, the processing included removal of nonbrain tissue using a hybrid watershed/surface deformation procedure; segmentation of subcortical white matter and deep gray matter structures, including the thalamus, hippocampus, amygdala, caudate, globus pallidum, putamen, and accumbens; motion correction; automated Talairach transformation;

TABLE 2. Cognitive Domains Tested, with the Tests Used and the Considered Variables in Each Test

Cognitive domains	Neuropsychological tests	Variables
Attention / working memory	Bells Cancellation test Hayling test and Trail Making test Wechsler Adult Intelligence Scale – III	Omissions (time 1) Errors (part A) Digits foward and backward and letter-number sequencing tasks
Memory (learning, recall)	Rey auditory verbal learning test	Mean of A1 and B1 trials; mean of A7, B1 and A5 trial
Sensory-perceptual and motor skills domains	Brazilian Brief Neuropsychological assessment battery (NEUPSILIN)	Constructive praxis task
Processing speed	Bells cancellation test Hayling test and Trail Making test	Omission (time 1) Time (part A)
Executive functions	Stroop test Trail Making test Hayling test	Color-word page; interference score Time (part B); errors (part B); Time B-Time A; Time B/Time A Errors part B; Time B-Time A
Verbal language	Montreal Communication Evaluation Battery	Semantic and phonemic verbal fluency tasks.

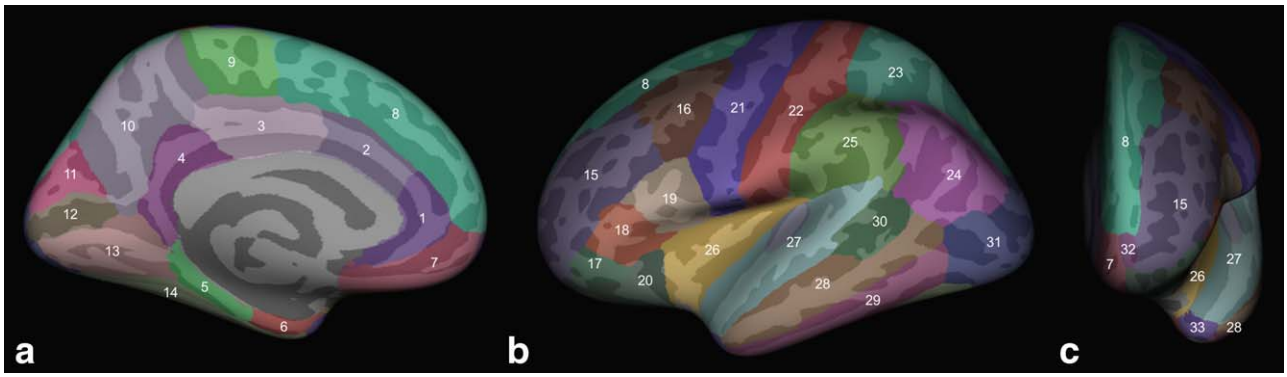

FIGURE 1: Cortical thickness was measured in cortical structures shown in this 3D rendering of the brain, from medial (a), lateral (b), and frontal (c) views. The cortical structures, considered by Freesurfer were rostral (1) and caudal (2) anterior cingulate gyri, posterior cingulate gyri (3), isthmus of cingulate gyri (4), parahippocampal gyri (5), entorhinal cortex (6), medial orbitofrontal cortex (7), superior frontal gyri (8), paracentral lobule (9), precuneus (10), cuneus (11), pericalcarine cortex (12), lingual gyri (13), fusiform gyri (14), rostral (15) and caudal (16) middle frontal gyri, pars orbitalis (17), pars triangularis (18) and pars opercularis (19) of inferior frontal gyri, lateral orbitofrontal cortex (20), precentral gyri (21), postcentral gyri (22), superior (23) and inferior (24) parietal cortex, supramarginal gyri (25), insular cortex (26), superior temporal gyri (27), middle temporal gyri (28), inferior temporal gyrus (29), banks of the superior temporal sulcus (30), lateral occipital cortex (31), frontal pole (32), and temporal pole (33).

normalization of intensity; tessellation of the gray matter/white matter boundary; automated topology correction; surface deformation following intensity gradients to optimally place the gray matter/white matter and gray matter/CSF borders at the location where the greatest shift in intensity defines these transitions; and inflation of the brain.

This method used both intensity and continuity information from the entire three dimensional MR volume in segmentation and deformation procedures to produce representations of cortical thickness, calculated as the closest distance from the gray matter/white matter boundary to the gray matter/CSF boundary at each vertex on the tessellated surface. Once an accurate white matter/gray matter surface had been created, the pial surface was generated by expanding the white matter surface, so that it closely followed the gray-CSF intensity gradient without crossing the white matter surface boundary. After the pial surface was generated, it was visually checked for defects that may have been created during automatic topology fixing. If the surface appeared to deviate from the gray matter-CSF boundary, manual editing was performed.

Cortical thickness maps were calculated for each subject. Mean cortical thickness was measured and statistically compared ($P < 0.05$) using the query design estimate contrast (QDEC) tool, a single-binary application in FreeSurfer software, which identifies group differences. Analysis of cortical thickness was adjusted for age and gender, using a smoothing factor of 10. FreeSurfer is hypothesis-free and can localize group differences in cortical thickness and volume data. All cortical regions were considered (Fig. 1). Corrections for multiple comparisons in cortical thickness data were performed by QDEC using Monte-Carlo simulation (significance set at $P < 0.05$), available in FreeSurfer.

Using the same technique, volumes of the following structures were measured automatically: thalamus, caudate, putamen, globus pallidum, accumbens, hippocampus, and amygdala. Next, volumes of these structures were corrected for head size by dividing each value by the intracranial volume (brain volume + CSF volume) and multiplying the result by 100. Statistical analyses were performed using miniTAB Statistical Software. Normality of deep gray matter volume distributions was tested using the Kolmogorov-Smirnov test. Differences in the volumes of deep gray matter structures were tested using Student's t-tests for paired samples (significance at $P < 0.05$). All comparisons were between the first and second MRIs within the same HIV-positive patients.

Postprocessing of White Matter Longitudinal Integrity Evaluation and Statistical Analysis

For voxelwise diffusion modeling, diffusion data were analyzed using FMRIB's Diffusion Toolbox within FSL 5.0 (http://www.fmrib.ox.ac.uk/fsl). After performing eddy current correction and brain extraction, FA images for all subjects were created by fitting a tensor model onto the raw diffusion data. Voxelwise statistical analysis of the FA data was carried out using Tract-Based Spatial Statistics (TBSS),[28] part of FSL. FA data for all subjects were aligned in a common space using the nonlinear registration tool FNIRT, which uses a b-spline representation of the registration warp field. Next, the mean FA image was created and thinned to create a mean FA skeleton, which represents the centers of all tracts common to the group. Aligned FA data for each subject were then projected onto this skeleton, and the resulting data were fed into voxelwise cross-subject statistics for all voxels with FA ≥ 0.30 to exclude peripheral tracts with significant inter-subject variability and/or partial volume effects with gray matter. By applying the original nonlinear registration of each subject's FA to standard space, the RD, MD, and axial diffusivity (AD) were also projected onto the mean FA skeleton.

To perform the longitudinal statistical analysis, differences were manually computed between the diffusion data (FA, RD, AD, and MD) for the first and corresponding second MRI for each subject. These difference values were then fed into a paired samples t-test by using permutation-based inference (5000 permutations), corrected for multiple comparisons (controlling the family wise error) with a threshold-free cluster enhancement (TFCE) and significance level of $P < 0.05$. The results were overlaid on the mean FA skeleton to identify possible altered areas in the main tracts using the Johns Hopkins University white matter tractography atlas and the

TABLE 3. Comparative Analysis among the First and Second MRIs of the HIV-Positive Patients*

Anatomical structures		First MRI (standard deviation)	Second MRI (standard deviation)	*P* value
Thalamus	left	0.430593061 (0.055144041)	0.428009232 (0.058021208)	0.8831
	right	0.418513902 (0.047219659)	0.413427973 (0.050280605)	0.7372
Caudate	left	0.210303509 (0.02105513)	0.20818835 (0.01883922)	0.7334
	right	0.227962044 (0.020635887)	0.227786565 (0.01994166)	0.9778
Putamen	left	0.366056132 (0.04735065)	0.348031789 (0.04060803)	0.1931
	right	0.350804334 (0.03817523)	0.341902771 (0.034981838)	0.4355
Globus Pallidum	left	0.103269907 (0.0129974)	0.096796811 (0.01366637)	0.1237
	right	0.100284384 (0.014590441)	0.097418198 (0.009308781)	0.4531
Accumbens	left	0.04178044 (0.008087721)	0.040624274 (0.008006665)	0.6441
	right	0.039552733 (0.007540999)	0.037976835 (0.008278162)	0.5227
Hippocampus	left	0.239784696 (0.032421248)	0.238010447 (0.029534906)	0.8539
	right	0.245437936 (0.031213469)	0.243943763 (0.025886466)	0.8602
Amygdala	left	0.094788464 (0.015556326)	0.095751117 (0.011434494)	0.8205
	right	0.105068328 (0.016020951)	0.103841291 (0.011573581)	0.7776

*There were no statistically significant differences in the volume of deep gray matter structures considered. Statistical analysis used: Student's t-tests for paired samples between the first and second MRIs.

International Consortium for Brain Mapping DTI-81 white matter labels atlas (JHU ICBM DTI-81), available within FSL.

Results

Cortical Thickness and Deep Gray Matter Structures Volume

Following the correction for multiple comparisons, no significant differences in cortical thickness were observed in the comparison between the first and second MRIs. There were no significant differences in the mean deep gray matter structures volumes, between the first and second MRIs too (Table 3).

White Matter Integrity

There were no significant differences in mean FA, RD, MD, or AD values of white matter tracts between the first and second MRI in HIV-positive patients (Fig. 2).

Discussion

This study used a voxel-based morphometry technique to longitudinally assess cortical thickness and deep gray matter volume and a voxelwise-based method to longitudinally assess DTI of white matter tracts in 21 HIV-positive patients on HAART with CD4+ T lymphocyte count >200 cells/mL, undetectable plasma viral load and no HIV-related dementia. Our results showed no differences in cortical thickness, deep gray matter volume, or diffusivity parameters between the first and second MRI, performed at an average interval of 26.6 months.

HAND can be divided into three groups[4] based on the presence of cognitive deficits measured by neuropsychological tests: asymptomatic neurocognitive impairment, mild neurocognitive disorder associated with HIV and HAD. By consensus, the cognitive domains tested are: verbal/language; attention/working memory; abstraction/executive functions; memory (learning; recall); speed of information processing; sensory-perceptual; and motor skills. Any of these cognitive abilities may be impaired in an HIV-positive population, and several domains can be impaired in the same individual.[29]

Memory deficits and executive dysfunction predominate in the post-HAART era.[30] These deficits can affect work and daily activities and may cause problems with medication adherence. The introduction of HAART changed the focus of HIV treatment from acute complications, which were usually opportunistic infections, to long-term complications, such as cardiovascular, renal, and CNS diseases. These complications are due to numerous factors, including the long-lasting inflammatory response to the HIV infection itself, HAART-related adverse events, host genetics, socioeconomic factors, and combinations of these factors.[26,31] Although there are insufficient data to determine the best therapeutic approach, HAART is apparently not sufficient to prevent or reverse HAND.[5,31] However, it appears to delay the onset and worsening of HAND, permitting HIV-infected individuals to live longer with the infection.[31] Similar to past neuropsychological studies, despite using HAART, the majority of participants in our study had some level of cognitive deficit with a predominant deficit in memory performances. Because HAART can delay HAND onset and worsening[31] and all the HIV-positive participants in this study were at HAART, maybe the absence of longitudinal differences in the imaging parameters assessed occurred because of the treatment.

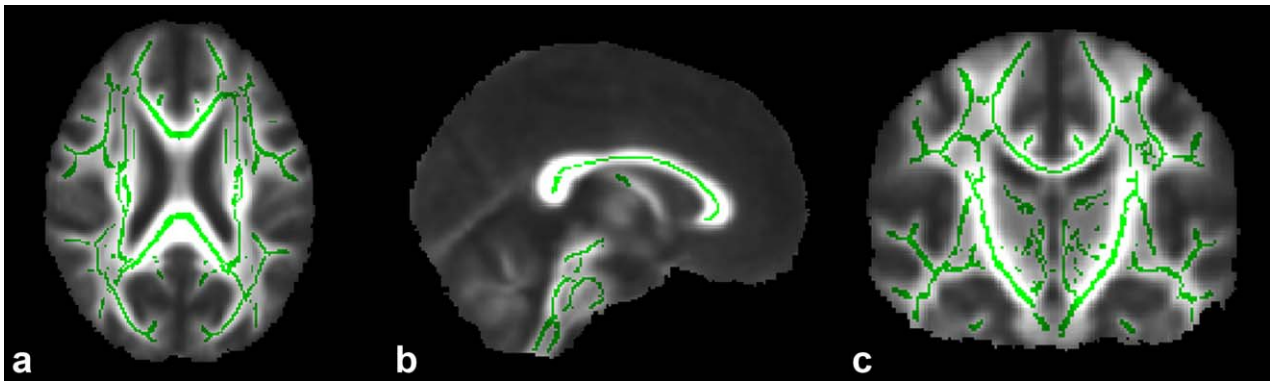

FIGURE 2: Corrected P maps show the voxels for the comparison of FA values between the first and second MRIs of the HIV-positive patients, in the axial (a), sagittal (b), and coronal (c) planes. Note that there is no statistically significant difference ($P < 0.05$) in the FA values in any voxel in this comparison, which would appear in red. Even before the correction for multiple comparisons, there were no significant differences in FA values, considering $P < 0.05$.

In a longitudinal study of early stage HIV-infected patients, Samuelsson et al[32] observed no decline in neuropsychological performance. MRI revealed that only a few patients had unspecific white matter lesions, mostly in subcortical regions, which were stable between examinations.

Previous cross-sectional studies have found diffuse brain atrophy in HIV-positive patients,[9,20–22] as well as smaller volumes of specific anatomical structures, such as the basal ganglia,[9] caudate,[20] putamen,[23] and total cortex.[22] Studies of cortical thickness in HIV-positive patients have shown atrophy in anterior cingulate and temporal cortices,[24] primary sensory and motor cortices, parietal association cortex, medial frontal and premotor cortex,[8] bilateral insula, orbitofrontal and temporal cortices, and right superior frontal cortex.[25] Several previous studies used DTI to assess white matter integrity in HIV-positive patients, showing decreased FA values in the genu,[11,19] splenium,[11,12] and body[7] of the corpus callosum, frontal white matter,[13] right posterior limb of the internal capsule, right inferior longitudinal fasciculus, and right optic radiation,[16] in all major white matter regions,[17] in the whole brain[14] in regions with nonspecific macrostructural lesions, encompassing several white matter tracts[18] and even no significant differences.[15] Studies that evaluated other diffusivity parameters in HIV-positive patients found increased RD and MD values in the genu,[19] splenium,[12] and body[7] of the corpus callosum, left posterior corona radiata,[7] and in all major white matter regions[17]; and increased AD values in the left superior corona radiata[7] and, to a lesser extent, in some white matter regions.[7,17] Unlike these previous cross-sectional studies, the aim of the current study was to evaluate longitudinal changes by comparing the same population of HIV-positive patients at two time points (mean interval of 26.6 months).

Other authors have found a significant effect of ageing in HIV-infected patients, independent of HIV-infection, in the superior temporal and inferior frontal regions and in the medial temporal and cingulate cortices,[33] fronto-temporal gray and white matter,[34] and caudate nucleus.[35] In a longitudinal study, Stout et al[36] found that accelerated ventricular volume enlargement and caudate nucleus volume reduction occurred in HIV-positive patients with CDC stage C disease, which was correlated with lower CD4+ T lymphocytes count. In the present study, HIV-positive patients did not show longitudinal changes in cortical thickness or deep gray matter volumes. The lack of differences in our study may have occurred because all patients were on stable HAART, had high CD4+ T lymphocyte counts and undetectable viral load, and none had HIV-related dementia. Similar to our study, Ances et al[35] did not find any longitudinal changes in basal ganglia, corpus callosum, or cortical volumes in patients on a stable HAART regimen who underwent two MRIs at a 6-month interval.

Using DTI in HIV-positive patients, Chang et al[37] found a significant increase in mean MD in the genu of the corpus callosum after one year. Although they found a trend for decreased FA in the putamen, no significant interactions between HIV-infection and time on FA values were observed in any brain regions. However, plasma viral load was undetectable in only 56% subjects at baseline MRI and in 62% subjects at follow-up MRI. Conversely, in the present longitudinal study, all HIV-positive patients had undetectable viral load at the time of both MRIs and did not show a significant change in DTI parameters, perhaps due to more effective treatment. In addition, Chang et al used a ROI-based technique to measure DTI parameters, which is susceptible to errors in positioning and does not assess all white matter tracts, and we used a voxel-based approach, which is less susceptible to positioning errors and evaluates all white matter tracts. Finally, although all patients in the study by Chang et al were receiving HAART, they did not specify the scheme used by each participant, and there could have been differences in antiretroviral CNS Penetration-Effectiveness Score in their study compared with the current study.

A limitation of this study is that our sample was too small to evaluate the longitudinal differences between patients without HAND and with asymptomatic and mild neurocognitive disorders. However, although there are neuropsychological tests to assess cognitive function, the analysis of daily activities performance is linked to educational, cultural and social trends, typically, using a self-report approach, in a subjective way. In addition, some studies show that existing HIV-associated neurocognitive disorders definitions for asymptomatic neurocognitive impairment and mild neurocognitive disorder might be too inclusive and lead to clinically inflation of impairment data.[38] Furthermore, some patients may fluctuate between non-HAND, asymptomatic neurocognitive impairment and mild neurocognitive disorder states.[38] So, our results were sufficient to demonstrate that HIV-positive patients without HAND or with asymptomatic and mild neurocognitive disorders did not present longitudinal worsening detectable by diffusivity measures, deep gray matter structures volumes and cortical thickness assessment. Also, we could not compare treated and untreated patients or different HAART schemes because all patients were on stable HAART. However, all HIV-positive patients enrolled in our study were homogeneously neurologically asymptomatic, without dementia, with a low viral load and high CD4+ T lymphocyte levels, reflecting the real-world clinical experience of most HIV-positive patients undergoing treatment. Although we have not included a control group in our study, it does not influence our results. Even though there is an age-related decline in gray matter volume[39] and DTI parameters[40] in healthy individuals, it is expected no significant longitudinal differences in these parameters in supposedly healthy individuals in an interval of 26.6 months.

In conclusion, assessment of cortical thickness, deep gray matter volume and DTI did not identify longitudinal differences in HIV-positive patients using HAART who had a stable infection status. This may be due to the efficacy of HAART, which cannot prevent HAND but can delay its onset and worsening. Other advanced MRI techniques, such as functional MRI, should be used in this population in the future to examine longitudinal effects of HIV-infection.

References

1. Valcour V, Chalermchai T, Sailasuta N, et al. Central nervous system viral invasion and inflammation during acute HIV infection. J Infect Dis 2012;206:275–282.
2. Valcour V, Sithinamsuwan P, Letendre S, Ances B. Pathogenesis of HIV in the central nervous system. Curr HIV/AIDS Rep 2011;8:54–61.
3. Chou SH, Prabhu SJ, Crothers K, Stern EJ, Godwin JD, Pipavath SN. Thoracic diseases associated with HIV infection in the era of antiretroviral therapy: clinical and imaging findings. Radiographics 2014;34:895–911.
4. Antinori A, Arendt G, Becker JT, et al. Updated research nosology for HIV-associated neurocognitive disorders. Neurology 2007;69:1789–1799.
5. Clifford DB. HIV-associated neurocognitive disease continues in the antiretroviral era. Top HIV Med 2008;16:94–98.
6. Spudich S, González-Scarano F. HIV-1-related central nervous system disease: current issues in pathogenesis, diagnosis, and treatment. Cold Spring Harb Perspect Med 2012;2:1–17.
7. Leite SC, Corrêa DG, Doring TM, et al. Diffusion tensor MRI evaluation of the corona radiata, cingulate gyri, and corpus callosum in HIV patients. J Magn Reson Imaging 2013;38:1488–1493.
8. Thompson PM, Dutton RA, Hayashi KM, et al. Thinning of the cerebral cortex visualized in HIV/AIDS reflects CD4+ T lymphocyte decline. Proc Natl Acad Sci U S A 2005;102:15647–15652.
9. Aylward EH, Henderer JD, McArthur JC, et al. Reduced basal ganglia volume in HIV-1-associated dementia: results from quantitative neuroimaging. Neurology 1993;43;2099–2104.
10. Dong O, Welsh RC, Chenevert TL, et al. Clinical applications of diffusion tensor imaging. J Magn Reson Imaging 2004;19:6–18.
11. Filippi CG, Ulug AM, Ryan E, Ferrando SJ, van Gorp W. Diffusion tensor imaging of HIV patients and normal-appearing white matter on MR images of the brain. AJNR Am J Neuroradiol 2001;22:277–283.
12. Wu Y, Storey P, Cohen BA, Epstein LG, Edelman RR, Ragin AB. Diffusion alterations in corpus callosum of patients with HIV. AJNR Am J Neuroradiol 2006;27:656–660.
13. Pomara N, Crandall DT, Choi SJ, Johnson G, Lim KO. White matter abnormalities in HIV-1infection: a diffusion tensor imaging study. Psychiatry Res 2001;106:15–24.
14. Ragin AB, Storey P, Cohen BA, Epstein LG, Edelman RR. Whole brain diffusion tensor imaging in HIV-associated cognitive impairment. AJNR Am J Neuroradiol 2004;25:195–200.
15. Ragin AB, Wu Y, Storey P, Cohen BA, Edelman RR, Epstein LG. Diffusion tensor imaging of subcortical brain injury in patients infected with human immunodeficiency virus. J Neurovirol 2005;11:292–298.
16. Gongvatana A, Schweinsburg BC, Taylor MJ, et al. White matter tract injury and cognitive impairment in human immunodeficiency virus–infected individuals. J Neurovirol 2009;15:187–195.
17. Chen Y, An H, Zun H, et al. White matter abnormalities revealed by diffusion tensor imaging in non-demented and demented HIV+ patients. Neuroimage 2009;47:1154–1162.
18. Stubbe-Dräger B, Deppe M, Mohammadi S, et al. Early microstructural white matter changes in patients with HIV: a diffusion tensor imaging study. BMC Neurol 2012;12:23.
19. Thurnher MM, Castillo M, Stadler A, Rieger A, Schmid B, Sundgren PC. Diffusion-tensor MR imaging of the brain in human immunodeficiency virus–positive patients. AJNR Am J Neuroradiol 2005;26:2275–2281.
20. Di Sclafani V, Mackay RD, Meyerhoff DJ, Norman D, Weiner MW, Fein G. Brain atrophy in HIV infection is more strongly associated with CDC clinical stage than with cognitive impairment. J Int Neuropsychol Soc 1997;3:276–287.
21. Patel SH, Kolson DL, Glosser G, et al. Correlation between percentage of brain parenchymal volume and neurocognitive performance in HIV-infected patients. AJNR Am J Neuroradiol 2002;23:543–549.
22. Ragin AB, Du H, Ochs R, et al. Structural brain alterations can be detected early in HIV infection. Neurology 2012;79:2328–2334.
23. Becker JT, Sanders J, Madsen SK, et al. Subcortical brain atrophy persists even in HAART-regulated HIV disease. Brain Imaging Behav 2011;5:77–85.
24. Küper M, Rabe K, Esser S, et al. Structural gray and white matter changes in patients with HIV. J Neurol 2011;258:1066–1075.
25. Kallianpur KJ, Kirk GR, Sailasuta N, et al. Regional cortical thinning associated with detectable levels of HIV DNA. Cereb Cortex 2012;22: 2065–2075.
26. Letendre SL, Ellis RJ, Everall I, Ances B, Bharti A, McCutchan JA. Neurologic complications of HIV disease and their treatment. Top HIV Med 2009;17:46–56.
27. Fischl B, Dale AM. Measuring the thickness of the human cerebral cortex from magnetic resonance images. Proc Natl Acad Sci U S A 2000;97:11050–11055.

28. Smith SM, Jenkinson M, Johansen-Berg H, et al. Tract-based spatial statistics: voxelwise analysis of multi-subject diffusion data. Neuroimage 2006;31:1487–1505.

29. Cañizares S, Cherner M, Ellis RJ. HIV and aging: effects on the central nervous system. Semin Neurol 2014;34:27–34.

30. Heaton RK, Franklin DR, Ellis RJ, et al. HIV-associated neurocognitive disorders before and during the era of combination antiretroviral therapy: differences in rates, nature, and predictors. J Neurovirol 2011;17:3–16.

31. Elbirt D, Mahlab-Guri K, Bezalel-Rosenberg S, Gill H, Attali M, Asher I. HIV-associated neurocognitive disorders (HAND). Isr Med Assoc J 2015;17:54–59.

32. Samuelsson K, Pirskanen-Matell R, Bremmer S, Hindmarsh T, Nilsson BY, Persson HE. The nervous system in early HIV infection: a prospective study through 7 years. Eur J Neurol 2006;13:283–291.

33. Becker JT, Maruca V, Kingsley LA, et al. Factors affecting brain structure in men with HIV disease in the post-HAART era. Neuroradiology 2012;54:113–121.

34. Towgood KJ, Pitkanen M, Kulasegaram R, et al. Mapping the brain in younger and older asymptomatic HIV-1 men: frontal volume changes in the absence of other cortical or diffusion tensor abnormalities. Cortex 2012;48:230–241.

35. Ances BM, Ortega M, Vaida F, Heaps J, Paul R. Independent effects of HIV, aging, and HAART on brain volumetric measures. J Acquir Immune Defic Syndr 2012;59:469–477.

36. Stout JC, Ellis RJ, Jernigan TL, et al. Progressive cerebral volume loss in human immunodeficiency virus infection: a longitudinal volumetric magnetic resonance imaging study. Arch Neurol 1998;55:161–168.

37. Chang L, Wong V, Nakama H, et al. Greater than age-related changes in brain diffusion of HIV patients after 1 year. J Neuroimmune Pharmacol 2008;3:265–274.

38. Clifford DB, Ances BM. HIV-associated neurocognitive disorder. Lancet Infect Dis 2013;13:976–986.

39. Inano S, Takao H, Hayashi N, et al. Effects of age and gender on neuroanatomical volumes. J Magn Reson Imaging 2013;37:1072–1076.

40. Madden DJ, Spaniol J, Costello MC, et al. Cerebral white matter integrity mediates adult age differences in cognitive performance. J Cogn Neurosci 2009;21:289–302.